Production of ultra-cold neutrons in solid α-oxygen

A Letters Journal Exploring the Frontiers of Physics

December 2011

EPL, **96** (2011) 62001 www.epljournal.org
doi: 10.1209/0295-5075/96/62001

Production of ultra-cold neutrons in solid α-oxygen

E. Gutsmiedl[1(a)], F. Böhle[1], A. Frei[1], A. Maier[1], S. Paul[1], A. Orecchini[2,3] and H. Schober[2]

[1] *Technische Universität München, Physik Department - James-Franck-Str. 1, D-85748 Garching, Germany, EU*
[2] *Institut Laue Langevin - 156X, F-38042 Grenoble CEDEX, France, EU*
[3] *Dipartimento di Fisica and CNR-IOM, Università di Perugia - I-06123 Perugia, Italy, EU*

received 6 April 2011; accepted in final form 26 October 2011
published online 1 December 2011

PACS 28.20.Cz – Neutron scattering
PACS 75.50.Ee – Antiferromagnetics

Abstract – Our recent neutron scattering measurements of phonons and magnons in solid α-oxygen have led us to a new understanding of the production mechanism of ultra-cold neutrons (UCN) in this super-thermal converter. The UCN production in solid α-oxygen is dominated by the excitation of phonons. The contribution of magnons to UCN production becomes only slightly important above $E > 10\,\mathrm{meV}$ and at $E \sim 4\,\mathrm{meV}$. Solid α-oxygen is in comparison to solid deuterium less efficient in the down-scattering of thermal or cold neutrons into the UCN energy regime. Nevertheless, the lower efficiency might be compensated by the larger mean free-path of UCN in oxygen with respect to deuterium.

Introduction. – Ultra-cold neutrons (UCN) are slow enough ($\sim 300\,\mathrm{neV}$) to be confined [1] in traps, which can be formed by materials with a high Fermi potential or by a magnetic field ($60\,\mathrm{neV/T}$). They can be kept for several minutes in the confinement, and thus be investigated with high precision. UCN are elementary particles that are extremely well suited for low-energy physics experiments. These experiments investigate fundamental problems unsolved within the framework of the Standard Model [2]. One major experiment is the search for a non-zero electric dipole moment of the neutron [3] (current upper limit $2.9 \cdot 10^{-26}\,\mathrm{e\,cm}$). Another unique experiment is the precise determination of the lifetime [4] of the free neutron. This value has an important impact on the theory of weak interactions [4,5].

Powerful UCN sources are needed for the experiments mentioned above in order to minimize the statistical errors, and different groups [6–9] are working on the development of strong UCN sources, based on solid deuterium (sD_2) as a converter for down-scattering of thermal or sub-thermal neutrons into the UCN energy region. Solid oxygen could be a valuable alternative when grown in the α-phase (α-sO_2). Solid α-sO_2 has a 2-dimensional antiferromagnetic structure [10], which exhibits, in addition to phonons spin wave excitations (magnons). This supplementary magnetic scattering of neutrons, considered for the first time by Liu and Young [11], might be a strong down-conversion channel, which would enhance the production of UCN. The achievable density of UCN in such a converter is described by

$$\rho_{UCN} = P_{UCN} \cdot \tau, \tag{1}$$

where P_{UCN} ($\mathrm{cm^{-3}\,s^{-1}}$) is the production rate of UCN and τ is the lifetime of UCN inside the converter. The lifetime τ of UCN in α-sO_2 is expected to be long ($\tau \simeq 375\,\mathrm{ms}$ at $T \leqslant 2\,\mathrm{K}$ [11]) compared to UCN lifetimes in solid ortho-deuterium ($\tau \simeq 20$–$30\,\mathrm{ms}$ at $T \leqslant 8\,\mathrm{K}$ [12]). A direct comparison of both converters, based on thermal and cold neutron scattering data, is shown in fig. 1. On the energy loss side (UCN production) sD_2 outperforms α-sO_2. This finding will be discussed more precisely further down in this paper. The cross-section of α-sO_2 on the energy gain side (UCN up-scattering) is very small compared to sD_2. This result is maybe a first confirmation of long lifetimes of UCN in α-sO_2, which leads to large mean free paths for UCN in the crystal.

Different groups [13–15] performed experiments concerning UCN production in such a converter. Their results are inconclusive and are a challenge to investigate α-sO_2 further. It seems that preparation of this cryo-solid is crucial [16]. Density inhomogeneities in α-sO_2 crystals may have an influence on the mean free path of the UCN. The exact knowledge of the inelastic scattering channels (energy loss and gain), deduced from neutron scattering data, in solid α-O_2 is therefore very important.

(a) E-mail: egutsmie@e18.physik.tu-muenchen.de

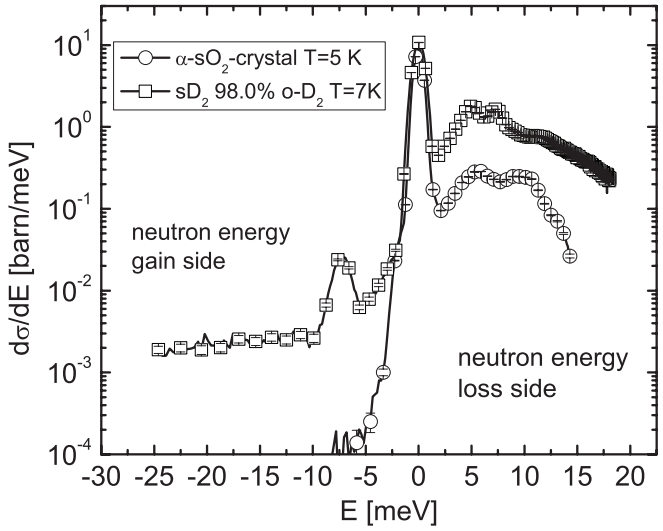

Fig. 1: $\mathrm{d}\sigma/\mathrm{d}E$ of α-sO_2 at $T = 5\,\mathrm{K}$ and solid deuterium [28] at $T = 7\,\mathrm{K}$.

Experimental results. – We have measured the phonon/magnon system in α-sO_2 by neutron time-of-flight (TOF) measurements at the IN4 spectrometer (Institute Laue-Langevin Grenoble —ILL). Thermal neutrons with an energy of $E_0 = 16.7\,\mathrm{meV}$ were used to determine the scattering function $S(Q, E)$ in the range 0–15 meV. The experimental setup (sample cell, gas system and slow control) was the same as that used in the measurements of the dynamical neutron scattering function of sD_2 [17]. We used oxygen gas with a purity $\geqslant 99.999\%$. Our measurements were performed without any external magnetic field. The α-sO_2 crystals were prepared from liquid via the γ- and β-phase [18]. The phase transition γ to β at $T = 43.8\,\mathrm{K}$ at vapor pressure was done in our experiments very slowly (10 mK/h) in order to get optical semi-transparent crystals. This procedure was developed in another experiment, performed in a special cryostat [16], which allowed us to watch the crystal growth by optical inspection through quartz windows.

The cross-section $\mathrm{d}\sigma/\mathrm{d}E$ of α-sO_2, the measured scattering function $S_{data}(Q, E)$ and the generalized density of states GDOS(E) are shown in figs. 1–3. Theoretical calculations [10,11,19] predict magnetic excitations in a broad energy band ($E \sim 1$–$20\,\mathrm{meV}$). At $E \simeq 10\,\mathrm{meV}$ a dominant delta-function–like peak should show up in the density of states (DOS) (see fig. 3 in [10]). This dominant peak sits on a broad distribution of states. The exact shape of this distribution is determined by values of the magnetic interaction parameters in α-sO_2. The magnon dispersions (acoustic and optic modes) possess an offset at $Q = 0\,\mathrm{Å}^{-1}$. Liu and Young [11] calculated a model scattering function $S(Q, E)$, which includes magnon-neutron scattering. Their scattering model shows significant scattering by magnons only at low Q values ($Q < 1\,\mathrm{Å}^{-1}$) on the energy loss side and thus they do not fall completely into the observational window of our experiment (see fig. 2). Magnon

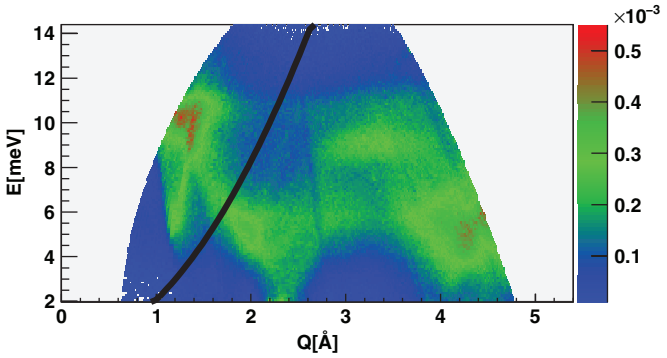

Fig. 2: $S(Q, E)$ (arbitrary units) of α-sO_2 at $T = 5\,\mathrm{K}$. Data from IN4 measurements. Black parabola: dispersion of the free neutron.

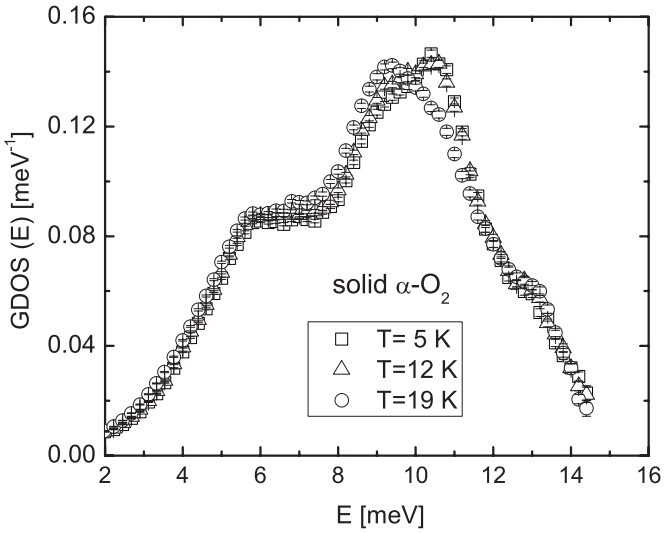

Fig. 3: Generalized density of states GDOS(E) of α-sO_2 at 5 K (□), 12 K (△), 19 K (◯). Data from IN4 measurements. GDOS is normalized to $\int_0^\infty \mathrm{GDOS}(E) \cdot \mathrm{d}E = 1$.

excitations at small Q values ($Q \mapsto 0\,\mathrm{Å}^{-1}$) [18,19] could in principle contribute to UCN production in α-sO_2. On the other hand, the results of Liu and Young are based on model input parameters affected by significant uncertainties. For completeness it would certainly be interesting to extend inelastic neutron scattering experiments to that low-Q region, or perform direct UCN production experiments with long-wavelength cold neutrons ($T_{eff} \ll 40\,\mathrm{K}$). The free-neutron parabola crosses this low-Q region only at energies smaller than $E = 2\,\mathrm{meV}$. It seems unlikely that the foreseen magnetic excitations can provide a significant contributions to UCN production, because the density of states for such magnons is quite small [10,20] for energies smaller than $E = 2\,\mathrm{meV}$. The cross-section $\mathrm{d}\sigma/\mathrm{d}E$ (see fig. 1) on the side of energy gain shows only up-scattering close to $E = 0$ (elastic peak). The up-scattering seen in our data is very likely due to phonons. This experimental observation should induce a large mean free path (λ_{mfp}) of UCN in α-sO_2, as predicted by Liu and Young [11].

Neutron scattering by solid oxygen is purely coherent and mostly elastic with $\sigma_{el}/\sigma_{tot} \sim 0.84$, as deduced from our neutron scattering data (see fig. 2). The elastic Bragg peaks in fig. 1 are cut out in order to enhance the contrast for the inelastic scattering in the plot.

The GDOS can be calculated from $S(Q,E)$ [21,22] by sampling over a large Q-range (neutron energy loss side) through the equation

$$\mathrm{GDOS}(E) = \left\langle E \cdot \frac{S(Q,E)}{Q^2 \cdot [n(E)+1]} \right\rangle_{2\theta}. \qquad (2)$$

The brackets $\langle \ldots \rangle_{2\theta}$ denote the average over all accessible scattering angles 2θ, while n is the Bose distribution for the phonons.

The GDOS(E) provides an estimate of the excitation spectra in the sample [23]. First values of the generalized density of states ($T \simeq 4\,\mathrm{K}$ and $23\,\mathrm{K}$) were published by [20] and [24]. Their results show a mixture of phonons, librons and antiferromagnetic excitations (magnons). The peak at $E \simeq 10.5\,\mathrm{meV}$ at $T = 5\,\mathrm{K}$ in our data is more pronounced as compared to the result of de Bernabe *et al.*, and the GDOS at $T = 10\,\mathrm{K}$ of [24] is closer to our result at $T = 5\,\mathrm{K}$. At higher temperatures, however, our GDOS and that reported [20] shows similar structures. Calculated contributions of magnons (see fig. 6 in [20]) should appear at $E \simeq 5\,\mathrm{meV}$ and $E \simeq 12.5\,\mathrm{meV}$, which are not detected in neither data sets. The magnon peak positions at lower energies are explained [20] by a decrease of the exchange constant (see eq. (6) in [20]) with decreasing temperature. A more detailed analysis of our neutron scattering data will be presented in a forthcoming paper.

UCN production cross-section. – The measurements in direct UCN production [13–15] experiments can be problematic, because it is difficult to disentangle UCN transport properties from UCN production (density inhomogeneities). These complications can be bypassed by using thermal or cold neutron scattering data for a direct determination of the production rate P_{UCN} of UCN in the converter. The uncertainty of this method is small compared to direct UCN production measurements. The experimental findings in our data have therefore an important impact on the UCN production in solid oxygen. The dynamical scattering function of solid oxygen resolved from our neutron scattering data has to be calibrated to absolute values. This calibration uses the known value of the total cross-section for thermal neutron energies:

$$\sigma_{tot}(E_0) = \int_0^\infty \mathrm{d}E_f \int \frac{k_f}{k_0} {b_{eff}}^2 S(Q,E)\,\mathrm{d}\Omega, \qquad (3)$$

where k_f and E_f are the wave vector and the energy of the scattered neutrons, respectively, while k_0 is the wave vector of the incident neutrons. The effective scattering length $b_{eff}^2 = 2 \cdot b_{nucl}^2 + b_{mag}^2$ [25] contains a combination of nuclear ($b_{nucl} = 5.8\,\mathrm{fm}$ [26]) and magnetic scattering ($b_{mag} = 5.38\,\mathrm{fm}$ [11]). The dynamical scattering function can be calculated via

$$S(Q,E) = \kappa \cdot S_{data}(Q,E). \qquad (4)$$

The value of the calibration factor $\kappa = 1240$ is obtained using eq. (3) and the total cross-section given by $\sigma_{tot}(E_0 = 16.7\,\mathrm{meV}) \approx 4\pi b_{eff}^2 = 12.1\,\mathrm{barn}$. The uncertainty of κ is in the order of $\Delta\kappa/\kappa \simeq 0.13$. This error was calculated, using the molecule form factors for nuclear and magnetic scattering. The uncertainty of κ at $E = 16.7\,\mathrm{meV}$ was determined by integrating the form factors over the solid angle and evaluating the variation of this values for different energy transfer $E \in (0\text{–}15\,\mathrm{meV})$. An additional uncertainty arises from the contribution of phonon and magnon excitations not covered by the limited kinematic range of the experiment (see fig. 2). We estimate a value of $\simeq 5\%$ for that uncertainty. The uncertainty of the total cross-section adds to approximately 18% (linear addition of uncertainties).

In the case of UCN production the following relations are valid: $E_f = E_U \ll E_0$; $E = E_0 - E_f \sim E_0$, where E_0 is the initial energy of the neutron before scattering. The UCN production cross-section can then be determined by direct integration of the dynamic neutron cross-section in the kinematic region along the free neutron dispersion parabola ($E_0 \approx \hbar^2 Q^2/2m$)

$$\sigma_{UCN}(E_0) = \int_0^{E_\mathrm{U}^{max}} \frac{\mathrm{d}\sigma(E_\mathrm{U})}{\mathrm{d}E_0} \mathrm{d}E_U. \qquad (5)$$

The evaluation of the integral (eq. (5)) uses the dynamic scattering function $S(Q, E = \frac{\hbar^2}{2m}k_0^2)$ at the phase space points of the neutron parabola. The UCN production cross-section can therefore be expressed by

$$\sigma_{UCN}(E_0) = \frac{\sigma_0}{k_0} S\left(k_0, \frac{\hbar^2}{2m}k_0^2\right) \frac{2}{3} k_U^{max} E_U^{max}. \qquad (6)$$

The term $E_0 = \frac{\hbar^2}{2m}k_0^2$ is the energy for an incoming neutron with wave vector k_0, whereas σ_0 is the total cross-section ($\sigma_0 = 4\pi b_{eff}^2$). The result for $\sigma_{UCN}(E)$ is shown in fig. 4. For comparison the UCN production cross-section for ortho-sD_2 is also included in fig. 4.

When determining the upper limit of the integration we also have to take into account that the UCN will gain kinetic energy when leaving the converter [27]. UCN produced in sD_2 gain $\Delta E_\mathrm{U} \sim 100$ neV, while for α-sO_2 $\Delta E_\mathrm{U} \sim 87$ neV. Therefore, the upper limit of the neutron energy inside the converters was set to $E_U^{max}(\alpha\text{-}sO_2) = 163\,\mathrm{neV}$ and $E_U^{max}(\text{ortho-}sD_2) = 150\,\mathrm{neV}$, respectively. These limits correspond to an upper limit of $E_U^{max} = 250\,\mathrm{neV}$ outside the converter (Fermi potential of UCN guide). The calculation of UCN production cross-section of sD_2 was performed using recently published data [28] for sD_2.

For α-sO_2 the dispersion parabola of the free neutron crosses a band of dispersive excitations at $E \sim 6\,\mathrm{meV}$ (see fig. 2). At this point the UCN production cross-section is

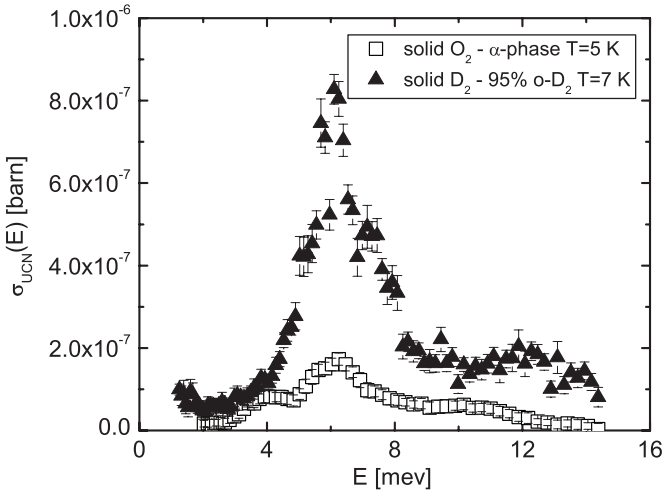

Fig. 4: UCN production cross-section of α-sO_2 (□) at $T = 5\,\mathrm{K}$ and sD_2 (95% ortho concentration) (▲) at $T = 7\,\mathrm{K}$ [12]. UCN energy range 0–150 neV inside the solid D_2, UCN energy range 0–163 neV inside the solid α-sO_2. Cross-sections determined by an integration of $S(Q, E)$ along the free dispersion of the neutron. Data from IN4 measurements.

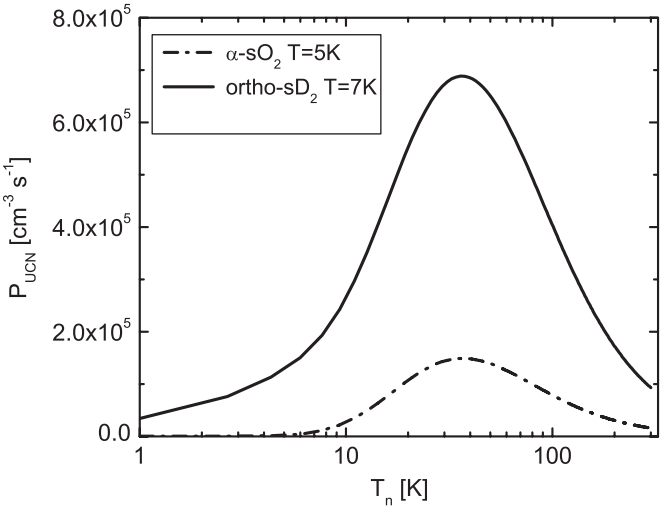

Fig. 5: Calculated UCN production rate of ortho-sD_2 at $T = 7\,\mathrm{K}$ (line) and α-sO_2 at $T = 5\,\mathrm{K}$ (dash-dotted line). Both converters are exposed to a neutron capture flux of $\Phi_C = 1 \cdot 10^{14}\,\mathrm{cm^{-2}\,s^{-1}}$ (Maxwellian shape with effective temperature $T_n \approx 40\,\mathrm{K}$).

determined by coherent phonon scattering. Therefore the major peak (fig. 4) at $E \sim 6\,\mathrm{meV}$ can be identified with the excitation of phonons (see also [19]). The structures in the UCN production cross-section at $E \sim 4\,\mathrm{meV}$ and $E \sim 10\,\mathrm{meV}$ are very likely induced by magnetic scattering (magnons) [20]. The contribution of magnons to the UCN production cross-section at $E \sim 4\,\mathrm{meV}$ and 10–12 meV is small compared to the phonon contribution at $E \sim 6\,\mathrm{meV}$. From our data we clearly conclude that the creation of phonons is the main energy loss channel in the conversion process of α-sO_2. α-sO_2 possesses a remarkably poorer capacity of creating UCN by down-scattering of thermal and sub-thermal neutrons as compared to solid ortho-deuterium (see fig. 4). This result can be explained by a larger inelastic cross-section of ortho-sD_2 ($T \simeq 7\,\mathrm{K}$) compared to α-sO_2 at thermal neutron energies [29]. The ratio of the two inelastic cross-sections is $\sigma_{inel}(\text{ortho-sD}_2)/\sigma_{inel}(\alpha\text{-sO}_2) \simeq 5.9$ at $E_0 = 16.7\,\mathrm{meV}$ (see fig. 1). On the other hand α-sO_2 should exhibit a large mean free path for UCN inside the converter as it is predicted by Liu and Young [11] and also indicated by our data (see fig. 1). Values up to $\lambda_{mfp} \simeq 4\,\mathrm{m}$ are expected. This opens the opportunity to construct a large UCN source with this material. Such a source could defeat a sD_2 source due to the small mean free path (several cm [6]) of UCN in solid deuterium. The analysis of our thermal neutron scattering data allows basically also the determination of the UCN up-scattering cross-section. The origin of this up-scattering is in this case purely inelastic and does not cover elastic scattering of UCN on density inhomogeneities in the crystals. This analysis is on-going and will be presented in a forthcoming paper.

The UCN production rate $P_{UCN}(\mathrm{UCN/cm^3\,s})$ of α-sO_2, which is exposed to a neutron spectrum $\mathrm{d}\Phi/\mathrm{d}E$ with Maxwellian energy distribution (T_n —effective temperature of the incoming neutron spectrum) can be calculated by

$$P_{UCN}(T_n) = N_{\mathrm{O_2}} \cdot \int_0^{E^{max}} \frac{\mathrm{d}\Phi(T_n)}{\mathrm{d}E_0} \cdot \sigma_{UCN}(E_0)\mathrm{d}E_0. \quad (7)$$

$N_{\mathrm{O_2}} = 2.9 \cdot 10^{22}\,\mathrm{cm^{-3}}$ is the particle density of O_2 molecules. Figure 5 shows the result for $P_{UCN}(T_n)$ for sD_2 and sO_2. Contrary to the results published in [11] (optimal $T_n \approx 10$–$15\,\mathrm{K}$) the UCN production rate has a maximum at $T_n \approx 40\,\mathrm{K}$. The uncertainty of P_{UCN} is determined by the error on σ_{UCN} ($\Delta\sigma_{UCN}/\sigma_{UCN} \simeq 0.18$).

Conclusion. – In summary, new neutron scattering data of solid α-oxygen lead to a better understanding of UCN production in this converter material. The new results for the UCN production cross-section, resolved directly from the dynamical scattering function $S(Q, E)$, show a significant UCN production cross-section for neutrons with energies at $E_0 \sim 6\,\mathrm{meV}$. Based on the identification of magnetic and vibrational excitations presented in Bernabe [20], the leading excitations are phonons and not magnons. This observation differs from numerical predictions [11] where contributions of magnons to the UCN production are assumed to be the leading process for UCN production in solid α-oxygen. Assuming energy modes outside the kinematic range of our scattering law measurements make negligible contributions to the inelastic scattering cross-section, an optimized α-sO_2 UCN source should be exposed to a cold-neutron flux with an effective neutron temperature of $T_n \simeq 40\,\mathrm{K}$, for which the production rate is maximal. At this temperature the UCN production rate in α-sO_2 is only 22% of the production rate of sD_2. A direct

comparison of a production rate deduced from UCN measurements [15] ($P_{UCN} \sim 2.2$–$2.4\,\mathrm{cm}^{-3} \cdot \mathrm{s}^{-1}$) with values ($P_{UCN} \sim 3.6\,\mathrm{cm}^{-3} \cdot \mathrm{s}^{-1}$) derived from neutron scattering data for a cold-neutron flux ($T_n \simeq 40\,\mathrm{K}$) of $\phi_{cold} \simeq 3.2 \cdot 10^9\,\mathrm{cm}^{-2} \cdot \mathrm{s}^{-1}$ in the sample shows a reasonable agreement. Finally it is worth mentioning that our data give some hints that the mean free path of UCN in solid α-oxygen might be large enough to allow to build a bigger source, which could compensate the small UCN production rate (compared to solid deuterium) in this converter.

* * *

This work was supported by the cluster of excellence "Origin and Structure of the Universe" (Exc 153) and by the Maier-Leibnitz-Laboratorium (MLL) of the Ludwig-Maximilians-Universität (LMU) and the Technische Universität München (TUM). We thank T. Deuschle, S. Materne, C. Morkel and H. Ruhland for their help during the experiments.

REFERENCES

[1] Golub R., Richardson D. and Lamoreaux S. K., *Ultra-Cold-Neutrons* (Adam Hilger, Bristol, Philadelphia, New York) 1991.
[2] Ramsey-Musolf M. J., *Nucl. Instrum. Methods Phys. Res. A*, **611** (2009) 111.
[3] Baker C. A. *et al.*, *Phys. Rev. Lett.*, **97** (2006) 131801.
[4] Paul S., *Nucl. Instrum. Methods Phys. Res. A*, **611** (2009) 157.
[5] Schreckenbach K., *J. Phys. G*, **14** (1988) S391.
[6] Frei A. *et al.*, *Eur. Phys. J. A*, **34** (2007) 119.
[7] Hill R. E. *et al.*, *Nucl. Instrum. Methods Phys. Res. A*, **440** (2000) 674.
[8] Anghel A. *et al.*, *Nucl. Instrum. Methods Phys. Res. A*, **611** (2009) 272.
[9] Serebrov A. *et al.*, *JETP Lett.*, **62** (1995) 785.
[10] Stephens P. W. and Majkrzak C. F., *Phys. Rev. B*, **33** (1986) 1.
[11] Liu C.-Y. and Young A. R., arXiv:nucl-th/0406004v1 (2004).
[12] Morris C. L. *et al.*, *Phys. Rev. Lett.*, **89** (2002) 272501.
[13] Atchison F. *et al.*, *EPL*, **95** (2011) 12001.
[14] Salvat D. *et al.*, *7th International UCN Workshop St. Petersburg Russia*, `http://cns.pnpi.spb.ru/ucn/index.html` (2009).
[15] Frei A. *et al.*, arXiv:1006.2970v2 [nucl-ex] (2011).
[16] Bozhanova Ralitsa, *Optical investigations of solid oxygen in the α-phase*, Bachelor Thesis, Technische Universität München, `http://www.e18.physik.tu-muenchen.de/`(2009).
[17] Frei A. *et al.*, *Phys. Rev. B*, **80** (2009) 064301.
[18] Freiman Yu. A. and Jodl H. J., *Phys. Rep.*, **401** (2004) 1.
[19] Jansen A. P. and van der Avoird A., *J. Chem. Phys.*, **86** (1987) 3583.
[20] de Bernabe A. *et al.*, *Phys. Rev. B*, **58** (1998) 14442.
[21] Squires G. L., *Introduction to the Theory of Thermal Neutron Scattering* (Cambridge University Press, Cambridge) 1978.
[22] Turchin V. F., *Slow Neutrons* (Israel Program for Scientific Translations, Jerusalem) 1965.
[23] Breuer N., *Z. Phys.*, **271** (1974) 289.
[24] Kilburn D. *et al.*, *Phys. Rev. B*, **78** (2008) 214304.
[25] The expression for b_{eff} is an approximation, which neglects interference effects (Melkonian E., *Phys. Rev.*, **76** (1949) 1750; Fermi E. and Marshall L., *Phys. Rev.* **71** (1947) 666) and nuclear and magnetic form factors (Sears V. F., *Can. J. Phys.* **44** (1966) 1279; Kleiner W. H., *Phys. Rev.*, **97** (1955) 411).
[26] `http://www.ncnr.nist.gov/resources/n-lengths/`.
[27] Altarev I. *et al.*, *Phys. Rev. Lett.*, **100** (2008) 014801.
[28] Frei A. *et al.*, *EPL*, **92** (2010) 62001.
[29] Atchison F. *et al.*, *Nucl. Instrum. Methods Phys. Res. A*, **611** (2009) 252.